Impact of Point Mutations on the Structure and Thermal Stability of Ribonuclease T1 in Aqueous Solution Probed by Fourier Transform Infrared Spectroscopy†

Heinz Fabian,*,‡ Christian Schultz,§ Jan Backmann,§ Ulrich Hahn,‖ Wolfram Saenger,⊥ Henry H. Mantsch,# and Dieter Naumann*,§

Institute for Biochemistry, Humboldt-University Berlin, c/o Max-Delbrück-Center for Molecular Medicine, Robert-Rössle-Strasse 10, D-13125 Berlin, FRG, Robert-Koch-Institute, Federal Health Office, Nordufer 20, D-13353 Berlin, FRG, Institute for Biochemistry, Medical University Lübeck, D-23538 Lübeck, FRG, Institute of Crystallography, Free University Berlin, Takustrasse 6, D-14195 Berlin, FRG, and Institute for Biodiagnostics, 435 Ellice Avenue, Winnipeg R3B 1Y6, Canada

Received May 23, 1994®

ABSTRACT: We undertook a detailed comparative analysis of the infrared spectra of wild-type ribonuclease T1 and three mutants: two single mutants, Tyr-45 → Trp (Y45W) and Trp-59 → Tyr (W59Y), and a double mutant, Tyr-45 → Trp/Trp-59 → Tyr (Y45W/W59Y). These mutants were selected because they are known to affect the activity of the enzyme. The structural differences were evaluated by using peptide backbone and side-chain "marker" bands as conformation-sensitive monitors. All mutations lead to a decrease of the thermal transition temperature, though the mutation Tyr-45 → Trp affects the T_m to a lesser degree than the replacement of Trp-59 by Tyr, both in the single (W59Y) and in the double (Y45W/W59Y) mutant. Small changes in the protein backbone conformation and in the microenvironment of certain amino acids, induced by the point mutations, could be detected. In particular, we found subtle differences in the hydrogen bonding pattern of the β-strands in the mutants W59Y and Y45W/W59Y, compared to that in wild-type RNase T1 and in the mutant Y45W. Practically identical spectra in the amide I region were obtained for the double mutant Y45W/W59Y and the single mutant W59Y, demonstrating that it is the change from Trp to Tyr in position 59 (located at the interface between the α-helix and a β-strand) which affects the overall protein conformation. The mutation Tyr to Trp in position 45, on the other hand, has practically no impact on the polypeptide backbone conformation. In addition, the mutation in position 59 also leads to changes in the microenvironment of (some) tyrosine residues, as revealed by the aromatic ring stretching vibration of tyrosine at 1516 cm^{-1}, a sensitive local monitor of protein conformation. The infrared results are correlated with X-ray data.

Ribonuclease T1 (RNase T1)[1] from *Aspergillus oryzae* is a small globular enzyme composed of 104 amino acids. It cleaves single-stranded RNA specifically at the 3′-phosphate of guanylic residues (Takahashi & Moore, 1982). The three-dimensional structure of RNase T1 is known, and genetically-engineered overproducers are available [for a review, see Pace et al. (1991)]. Various X-ray studies have shown that the secondary structure of RNase T1 includes a long α-helix, a major antiparallel β-sheet composed of three long and two short β-strands, a short two-stranded antiparallel β-sheet close to the N-terminus of the protein, and four wide loops which include several types of turns (see Figure 1).

Recent kinetic studies of wild-type RNase T1 and a number of its mutants showed that the replacement of the only tryptophan in RNase T1, Trp-59, by tyrosine, has a particularly strong effect on the activity of the enzyme (Grunert et al., 1993). Since tryptophan-59 is sequentially adjacent to Glu-58, a residue intimately involved in the catalytic process, it seems likely that structural changes induced by the mutation W59Y alter the geometry of the active site, thereby accounting for the observed changes in enzymatic activity. In addition, the exchange of tryptophan for the smaller sized tyrosine in position 59, located at the interface between the α-helix and a β-strand (Figure 1), may also have an impact on the overall conformation of RNase T1.

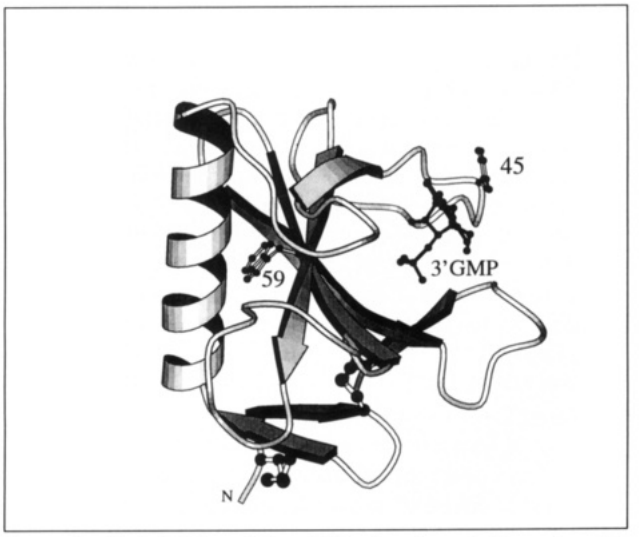

FIGURE 1: Pictorial description of the structure of ribonuclease T1 and 3′-guanylic acid as substrate. The mutation sites are indicated by including the side chains of the substituted residues as a ball and stick representation. The plot was drawn with the MOLSCRIPT program (Kraulis, 1991).

† This work was supported by grants from the Deutsche Forschungsgemeinschaft (to D.N., U.H., and W.S.) and by the Fonds der Chemischen Industrie (to W.S.). Issued as NRCC Publication No. 34742. H.F. thanks the A. v. Humboldt Foundation, Bonn, for a Feodor Lynen Research Fellowship.

‡ Humboldt-University Berlin.
§ Robert-Koch-Institute.
‖ Medical University Lübeck.
⊥ Free University Berlin.
Institute for Biodiagnostics.

® Abstract published in *Advance ACS Abstracts,* August 1, 1994.

[1] Abbreviations: RNase T1, ribonuclease T1; FT-IR, Fourier transform infrared.

0006-2960/94/0433-10725$04.50/0

To investigate possible effects of such mutations on the structure and the stability of RNase T1 in aqueous solution, the infrared spectra of three mutants (W59Y, Y45W, and Y45W/W59Y) were compared with those of the wild-type protein. Notwithstanding certain limitations (Surewicz et al., 1993), Fourier transform infrared (FT-IR) spectroscopy is becoming an increasingly valued tool for examining protein secondary structures in solution. We recently reported an investigation of wild-type RNase T1 (Fabian et al., 1993). Under our experimental conditions, the protein did not aggregate, and the complete reversibility of the thermal unfolding permitted a detailed description of the structural changes that occur as a function of temperature. Herein, we discuss the effect of point mutations on the structure and stability of this protein. Furthermore, subtle structural differences between the folded state of wild-type RNase T1 and those of certain mutants were scrutinized by infrared difference spectroscopy. The observation of albeit minor changes in protein structure by infrared difference spectroscopy can provide information about changes in single amino acids; so far this had been limited to studies with light-triggered chromophoric proteins whose spectra can be obtained with minimal sample manipulation and without removing it from the instrument [for a review, see Braiman and Rothschild (1988)]. The quantitative comparison of spectra of different samples, often recorded at different protein concentrations, requires an internal standard for their normalization. In the case of RNase T1, the infrared spectra of the thermally unfolded proteins, which all exhibited broad and practically identical amide I band contours, turned out to provide an excellent intensity standard for the quantitative comparison of the spectra of the corresponding native proteins.

MATERIALS AND METHODS

Proteins. Recombinant wild-type Lys25-RNase T1 was expressed using the pA2T1 vector system and purified as described (Landt et al., 1992). The mutants W59Y, Y45W, and Y45W/W59Y were produced by site-directed mutagenesis using the polymerase chain reaction, and isolated from an *Escherichia coli* overproducing clone (Landt et al., 1990). To obtain defined buffer conditions for the infrared measurements, the lyophilized samples were dissolved, filtered at diluted buffer conditions through Sephadex G25, and lyophilized again. Prior to the infrared experiments, the samples were dissolved in the appropriate volumes of ^2H_2O to yield buffer conditions of 10 mM sodium cacodylate at pD 7.0, and protein concentrations of 10–15 $\mu g \cdot \mu L^{-1}$. The reference peptide T-T-N-Y-T was a generous gift of Dr. L. Ötvös, Jr., Philadelphia.

Infrared Spectroscopy. Infrared spectra were recorded with two types of instruments. FT-IR measurements at discrete temperatures were performed using a Digilab FTS-40A spectrometer equipped with a liquid nitrogen cooled MCT detector and continuously purged with dry air. The protein solutons (15 μL) were placed between a pair of CaF_2 windows separated by a path length of 45 μm. For proper compensation of ^2H_2O absorption, the buffer solutions were measured in a cell with a slightly shorter path length. The sample temperature was controlled by means of a thermostated cell jacket. To obtain spectra at discrete temperatures, the protein solutions were heated from 20 to 70 °C in intervals of 5 °C. Spectra obtained at these temperatures were recorded by equilibrating the sample for 10 min prior to data collection which itself took 6 min. For each sample, 512 interferograms were co-added and Fourier-transformed to yield spectra with a nominal resolution of 2 cm^{-1}. The protein spectrum was obtained by subtracting the ^2H_2O–buffer spectrum from the spectrum of the protein solution measured at the same temperature. Spectral contributions from residual water vapor were eliminated using a set of water vapor spectra, as described earlier (Fabian et al., 1993). The final unsmoothed protein spectra were used for further analysis.

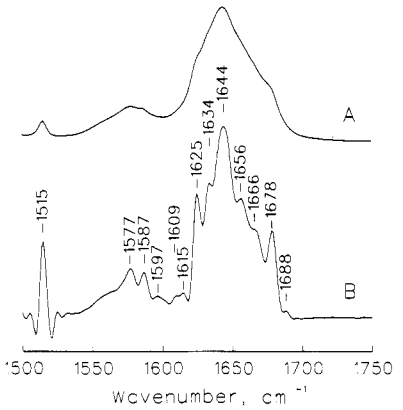

FIGURE 2: (A) Original infrared spectrum of the mutant Y45W/W59Y in ^2H_2O–buffer solution at room temperature. (B) Infrared spectrum of the mutant Y45W/W59Y after band-narrowing by Fourier self-deconvolution (see Materials and Methods for details).

For temperature profile measurements, FT-IR spectra were collected continuously on a Bruker IFS-66 FT-IR spectrometer equipped with a DTGS detector. The temperature of the gas-tight IR cell device was linearly increased at a rate of 0.5 $°C \cdot min^{-1}$ while recording 227 interferograms per 1 °C change in temperature. The path length of the IR cell was 50 μm. Infrared spectra of the protein solutions and the buffer solution were measured using the same temperature gradient. All protein spectra were corrected for the contributions of buffer and residual water vapor as described for the measurements at discrete temperatures. Band-narrowing by Fourier self-deconvolution was performed as described previously (Mantsch et al., 1988) using a half-bandwidth of 15 cm^{-1} and a band-narrowing factor $k = 2.0$. The evaluation of band maxima for frequency/temperature plots was performed using a center-of-gravity algorithm (Cameron et al., 1982).

RESULTS

Assignment of Infrared Bands Figure 2A shows a representative infrared spectrum of the mutant Y45W/W59Y in ^2H_2O–buffer solution after complete ^1H–^2H exchange and subtration of the buffer. Complete N^1H–N^2H exchange was achieved by keeping the protein solutions for 30 min at a temperature a few degrees below the denaturation temperature (Fabian et al., 1993). At room temperature, the original spectra of the mutants Y45W/W59Y, Y45W, and W59Y are very similar to those of the wild-type protein. The prominent band centered at 1644 cm^{-1} is due to the conformation-sensitive amide I mode [essentially comprising the C=O stretching vibratin of all the amide groups (Miyazawa & Blout, 1961)], while the bands between 1515 and 1615 cm^{-1} (in fully ^1H–^2H exchanged proteins) are entirely due to amino acid side-chain absorptions: tyrosine (1515 and 1615 cm^{-1}), glutamate (1577 cm^{-1}), aspartate (1587 cm^{-1}), and arginine (1597 and 1609 cm^{-1}) (Chirgadze et al., 1975).

As for many other proteins, the amide I band contour is a composite of several overlapping components. Most of these component bands can be resolved by Fourier self-deconvolution, such as shown in Figure 2B for the spectrum of the mutant Y45W/W59Y. The amide I band components in the deconvoluted infrared spectra of the native protein have

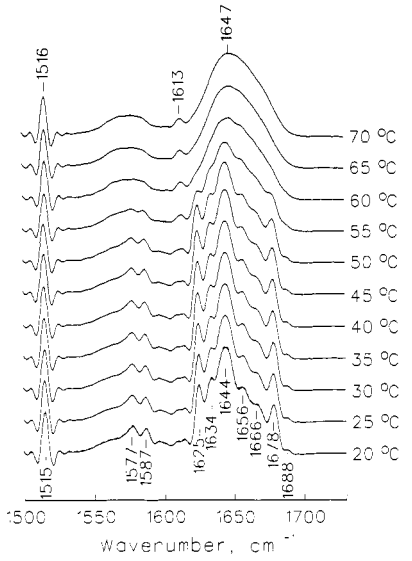

FIGURE 3: Infrared spectra of the mutant Y45W/W59Y in ^2H_2O–buffer at the indicated temperatures. All spectra are shown after Fourier self-deconvolution. Note that the spectra obtained at 20 °C before heating (solid line at 20 °C) and after cooling from 70 °C down to 20 °C (dashed line at 20 °C) are practically identical.

previously been assigned to characteristic secondary structure elements: the infrared bands at 1625 and 1634 cm^{-1} to different β-sheet structures and the band at 1656 cm^{-1} to the α-helix. The component at 1644 cm^{-1} was assigned to irregular structures with minor contributions from 3_{10}-helical and/or β-turn structures all present in RNase T1. The band at 1666 cm^{-1} was attributed to turn structures; turns and antiparallel β-sheet structures were associated with the band components at 1678 and 1688 cm^{-1} (Fabian et al., 1993).

Effect of Point Mutations on the Thermal Stability of RNase T1 and the Thermodynamics of Unfolding. Figure 3 shows infrared spectra of the mutant Y45W/W59Y in ^2H_2O–buffer recorded between 20 and 70 °C in intervals of 5 °C. The temperature study of all proteins was carried out after complete N^1H–N^2H exchange; therefore, the spectral changes observed as a function of temperature solely reflect structural changes due to the thermal unfolding of the protein. The spectra measured between 20 and 50 °C are very similar to each other, indicating no or merely minor changes in the secondary structure over this temperature range. On the other hand, the spectra measured between 50 and 60 °C are quite different, demonstrating that major structural changes occur over this temperature range. The spectrum after complete thermal denaturation, at 70 °C, exhibits only a broad, nearly featureless amide I band contour centered at 1647 cm^{-1}. Practically identical amide I band contours were obtained for the thermally unfolded state of all RNase T1 mutants, as well as for the wild-type protein; these contours are typical of predominantly, but not completely, irregular protein structures. Residual, turnlike structures were suggested to exist in the unfolded state of wild-type RNase T1 (Fabian et al., 1993). The spectrum obtained after cooling the protein sample from 70 °C down to 20 °C was practically identical to the spectrum before heating. The same applies to the mutants Y45W and W59Y. This indicates that the thermal unfolding of these proteins is reversible even at the relatively high protein concentrations used here. Other proteins, such as concanavalin A (Arrondo et al., 1988) or cytochrome *c* (Muga et al., 1991), showed irreversible intermolecular β-aggregation upon thermal denaturation, as demonstrated by the appearance of a strong infrared band at ~1618 cm^{-1}. The present results obtained

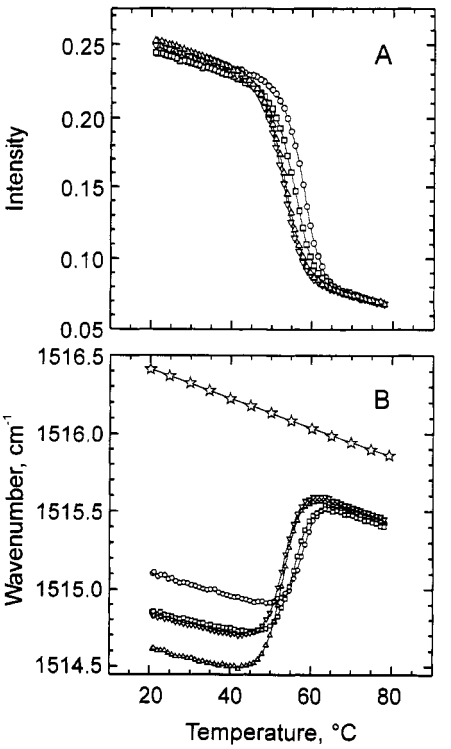

FIGURE 4: Temperature dependence of the peak height intensity of the amide I band at 1625 cm^{-1} (A) and temperature dependence of the position of the tyrosine band (B) for wild-type RNase T1 (○) and for the mutants Y45W/W59Y (△), W59Y (▽), and Y45W (□). The upper trace in Figure 4B (☆) shows the temperature dependence of the position of the tyrosine band from the single tyrosine residue in a short peptide with the sequence T-T-N-Y-T, known to lack any secondary structure at all temperatures.

with RNase T1, along with a recent infrared study of RNase A (Yamamoto & Tasumi, 1991), clearly show that irreversible β-aggregation of proteins at high temperatures and at high protein concentrations is not necessarily the rule, but likely an intrinsic property of those proteins that show it.

In a second type of experiments, infrared spectra were collected along a linear temperature gradient of 0.5 °C·min^{-1} by ramping up the temperature from 21 to 78 °C. From these data, intensity/temperature and frequency/temperature profiles for selected infrared "marker" bands were constructed. The various mutant spectra measured at 78 °C, which all exhibited nearly identical amide I band contours, provided the intensity standard necessary for comparison with the respective spectra of the folded proteins. Figure 4A shows intensity/temperature plots for the amide I component at 1625 cm^{-1} (β-strands) in the spectra of wild-type RNase T1 and in the mutants Y45W/W59Y, W59Y, and Y45W. This band exhibits the strongest temperature-dependent absorbance changes among the various amide I band components and therefore provides a good monitor for the thermal unfolding of the secondary structure of the different RNase T1 mutants.

The temperature-induced unfolding of proteins not only involves the breakdown of the various secondary structural elements but also leads to changes in the microenvironment of side-chain groups. A side-chain vibration that can be distinguished particularly well in the spectra of proteins in ^2H_2O is the aromatic ring stretching vibration of tyrosine, at 1516 cm^{-1}. The position of this band is sensitive to the protein conformation (Arrondo et al., 1988; Fabian et al., 1993). Since changes in the environment of tyrosine residues may result from changes in both tertiary and secondary structure, the tyrosine band at 1516 cm^{-1} provides a specific local monitor

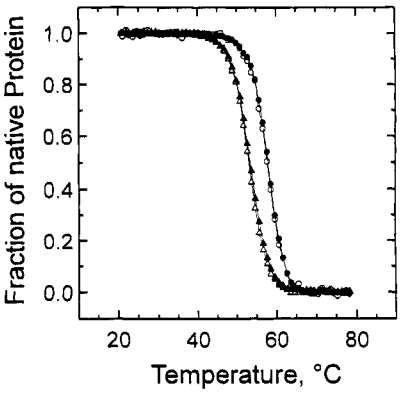

FIGURE 5: Fraction of native protein in wild-type RNase T1 (circles) and in the mutant Y45W/W59Y (triangles) as a function of temperature, as estimated from the infrared "marker" bands shown in Figure 4A,B (closed symbols as obtained from the β-band; open symbols as obtained from the corresponding Tyr band).

Table 1: Transition Temperatures (T_m)[a] and van't Hoff Enthalpies (ΔH) as Calculated either from the Intensity/Temperature Plot of the β-Band at 1625 cm^{-1} or from the Frequency/Temperature Changes of the Tyrosine Ring Vibration at 1516 cm^{-1}

RNase T1	wild-type	Y45W/W59Y	W59Y	Y45W
		β-Band		
T_m (°C)[b]	57.6	53.1	53.4	56.0
ΔH (kJ·mol^{-1})[c]	416	374	370	373
		Tyr Band		
T_m (°C)[b]	57.6	52.9	53.1	55.7
ΔH (kJ·mol^{-1})[c]	416	391	385	397

[a] T_m and ΔH values were calculated from the infrared data as described earlier (Fabian et al., 1993). [b] The uncertainty of the T_m value estimation is ±0.2 °C. [c] The uncertainty of the ΔH value estimation is ±20 kJ·mol^{-1}.

for such conformational changes. Figure 4B shows frequency/temperature plots for the tyrosine band in wild-type RNase T1 and in the three mutants. The transition curves given in Figure 4A and Figure 4B were also used to determine the respective transition temperatures (T_m) and to compute enthalpy changes (ΔH), assuming that the protein unfolding follows a two-state transition between the folded and the unfolded state (see Figure 5 and Table 1).

Several conclusions can be drawn from the data in Figures 4 and 5 and Table 1: (i) The thermal unfolding begins earlier in each of the investigated mutants. The T_m value for the mutant Y45W/W59Y is 4.7 °C lower compared to that of wild-type RNase T1, demonstrating that the double mutation clearly affects the thermal stability of RNase T1. However, the fact that almost identical T_m values were obtained for the double mutant Y45W/W59Y and the single mutant W59Y demonstrates that it is the change from tryptophan to tyrosine in position 59 which effects the thermal unfolding of the protein. The replacement of Tyr-45 by a tryptophan residue has little effect on the thermal stability of RNase T1; the transition temperature is only 1.8 °C lower when compared to that of the wild-type protein . (ii) The transition temperatures and transition profiles derived from the temperature dependence of the two infrared "marker" bands are very similar for a given mutant. This indicates a simultaneous breakdown of secondary structure elements and pronounced changes in the microenvironment of side-chain groups (as illustrated in Figure 5 for β-structures and tyrosine residues), suggesting a highly cooperative unfolding process. The ΔH values obtained for the three mutants are slightly lower than those estimated for the wild-type protein, suggesting a somewhat lower cooperativity of the thermal unfolding of all three mutants. The ΔH value of 416 kJ·mol^{-1} for wild-type RNAse T1 derived from the present infrared data is in excellent agreement with the value of 412 kJ·mol^{-1} obtained recently under comparable experimental conditions by differential scanning calorimetry (Yu et al., 1994). On the other hand, not unexpectedly, the T_m value obtained here for the wild-type RNAse T1 in D_2O–buffer is about 4.5 °C higher than that derived from the calorimetric data in H_2O–buffer (Plaza del Pino et al., 1992; Yu et al., 1994). It is well-known that proteins in D_2O solutions show higher T_m values compared to those found in H_2O solutions (Talluri & Scheraga, 1990; Yamamoto & Tasumi, 1991). More importantly, however, the relative differences between the T_m values for the wild-type RNase T1 and the three mutants determined by infrared spectroscopy in D_2O–buffer are in good agreement with the corresponding differences between the T_m values derived from scanning calorimetric data obtained in H_2O–buffer (Schubert et al., 1994). (iii) While the spectrum of the wild-type protein at 70 °C is practically identical with that of the mutant Y45W/W59Y, their spectra at 21 °C show minor differences, particularly with respect to the position of the tyrosine band (see Figure 4B). This indicates that under ambient conditions there are subtle conformational differences between the wild-type protein and the mutant Y45W/W59Y. At 78 °C, the position of the tyrosine band is practically the same in the spectra of wild-type RNase T1 and all the mutants, but different from that of the corresponding tyrosine band in the spectrum of a structureless peptide, also measured at 78 °C (upper trace in Figure 4B). This reference peptide contains only a single tyrosine residue in position 4 of the sequence T-T-N-Y-T. This suggests that, on the average, the microenvironment of the tyrosine residues in all RNase T1 samples in the unfolded state is very similar, but (at least for some residues) different from that of a tyrosine residue in a peptide segment with no structure and with the particular amino acid sequence of this reference peptide. The reference peptide shows only a gradual, 0.5 cm^{-1}, downshift of the tyrosine frequency upon raising the temperature from 20 to 80 °C. Since the peptide lacks any regular structure at all temperatures, this shift must reflect a general effect of temperature on the frequency of the tyrosine band. A similar, gradual downshift of the tyrosine frequency is also observed for wild-type RNase T1 and the three mutants between 21 and 50 °C, that is, as long as the secondary structure of RNase T1 is essentially retained. However, the wavenumber position of the tyrosine ring vibration is 1.4–1.9 cm^{-1} lower in the RNase T1 samples compared to that in the reference peptide. Furthermore, at the corresponding denaturation temperatures of the proteins, there is a pronounced, discontinuous high-frequency shift of the tyrosine ring vibration, not observed for the reference peptide. The latter demonstrates that the changes in the tyrosine frequency at T_m indeed reflect conformational changes in RNase T1 and that the aromatic ring stretching vibration of tyrosine can be used as a sensitive local monitor of protein conformation (likely from both tertiary and secondary structural changes). It then follows that the 0.5 cm^{-1} difference in frequency at 21 °C (1515.1 cm^{-1} in the wild-type and 1514.6 cm^{-1} in the double mutant) must reflect subtle differences in the microenvironment of (at least some) tyrosine residues.

DISCUSSION

Infrared Difference Spectroscopy and Comparison with X-ray Data. In order to detect fine differences between the wild-type RNase T1 and its mutants, we have resorted to infrared difference spectra. The lower panel (A) in Figure

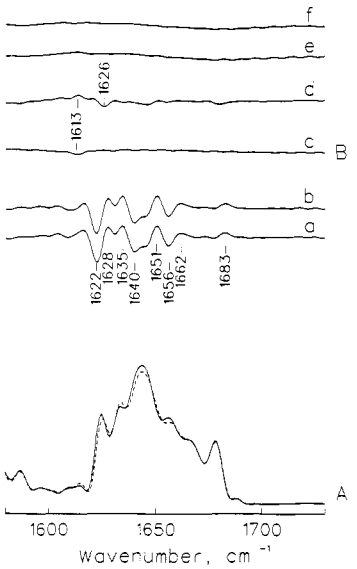

FIGURE 6: (A, bottom panel) Deconvolved infrared spectra of wild-type RNase T1 (dashed line) and of the mutant Y45W/W59Y (solid line) at 20 °C after normalization using the spectra of the corresponding thermally unfolded proteins. (B, top panel) Infrared difference spectra: (a) wild-type at 20 °C minus Y45W/W59Y mutant at 20 °C; (b) wild-type at 20 °C minus W59Y mutant at 20 °C; (c) Y45W/W59Y mutant at 20 °C minus W59Y mutant at 20 °C; (d) wild-type at 20 °C minus Y45W mutant at 20 °C; (e) wild-type at 70 °C minus Y45W mutant at 70 °C; (f) wild-type at 70 °C minus Y45W/W59Y mutant at 70 °C. Note that the absorbance scale for the difference spectra in part B was expanded by a factor of 2 compared to the scale in part A.

6 shows the infrared absorbance spectra of wild-type RNase T1 (dashed line) and the mutant Y45W/W59Y (solid line) after normalization by use of the respective infrared spectra of the thermally unfolded proteins. The upper panel (B) in Figure 6 shows infrared difference spectra between the wild-type protein and the various mutants. Positive and negative features in these difference spectra reflect fine structural differences, in whose absence only a flat line is obtained. This is illustrated by the flat difference spectra obtained from the thermally denatured proteins recorded at 70 °C (traces e and f in Figure 6) which also demonstrate the high stability of the instrument. The high signal-to-noise ratio of the absorbance spectra (>10 000:1) allowed us to compute differences between deconvolved spectra which provide considerable more details than difference spectra obtained from the original spectra.

There are clear spectral differences at 20 °C between wild-type RNase T1 on the one hand, and the two mutants Y45W/W59Y and W59Y, on the other hand (traces a and b, respectively in Figure 6). The positive bands at 1628 and 1635 cm^{-1}, along with the negative band at 1622 cm^{-1}, in these infrared difference spectra reflect fine differences in the hydrogen-bonding pattern of the β-type structures in the two mutants, compared to that of the wild-type protein. The interpretation of the other spectral differences above 1635 cm^{-1} is more complex and involves different types of structural elements. The negative bands at 1656 cm^{-1} (assigned to the α-helix) and at 1640 cm^{-1} (assigned to 3_{10}-helical and/or β-turn structures) suggest that in the two mutants there are more amide groups present in these structural elements. The positive bands at 1651, 1662, and 1683 cm^{-1}, on the other side, point to a higher percentage of irregular and turn structures in wild-type RNase T1. However, whether the minor spectral differences above 1635 cm^{-1} indeed reflect the suggested structural changes or in fact represent only minor differences in the spatial arrangement of existing structural elements, which thus affect their intrinsic absorptivities, cannot be easily answered by infrared spectroscopy.

A comparison of the X-ray structures (at a resolution of 0.23 nm) of enzyme–inhibitor complexes shows that the replacement of Trp-59 to Tyr leads to a 0.04 nm shift of the single α-helix (residues 13–29) toward the β-sheet, as well as to differences in the active-site geometry (i.e., in the loops defined by residues 33–37, 43–45, 48–52, and 70–75) (Schubert el al., 1994). Such structural distortions, if also present in aqueous solution, may account for the observed spectral differences. On the other hand, no differences in the hydrogen-bonding pattern of the β-strands, such as suggested by the infrared data, are evident from the X-ray data. This suggests either that the proposed distortions of β-strands are too small to be detected by X-ray diffraction at 0.23 nm resolution or that they are absent in the crystalline state and only present in aqueous solution. The X-ray data, however, show a string of water molecules between the α-helix and the β-sheet, bound to the Nϵ1 of Trp-59 in the wild-type protein. This string of water molecules is disturbed by the replacement of Trp-59 with Tyr, because tyrosine does not have a hydrogen-bond donor in a position comparable to that of Nϵ1 in tryptophan. The ensuing changes in the structure of the bound water in this region can impact on the conformation of the β-strands, which in turn may cause the spectral changes discussed above. The fact that discrete backbone changes are detected at all by infrared difference spectroscopy reflects the sensitivity of this technique to changes in the hydrogen-bonding pattern of β-strands. The fact that the spectrum of the double mutant and that of the single mutant are practically identical (trace c in Figure 6 is essentially flat) demonstrates that it is the change from tryptophan to tyrosine in position 59 which affects the overall protein conformation. The mutation of tyrosine to tryptophan in position 45 has little effect on the secondary structure, as indicated by the minor differences between the spectra (trace d in Figure 6); this is in good agreement with earlier X-ray data on this mutant (Koellner et al., 1991; Itoh et at., 1991). The conformational changes induced by the mutation in position 45 are essentially restricted to the substrate recognition site of the enzyme; they have practically no impact on the polypeptide backbone conformation, and thus leave the amide I band characteristics almost unchanged.

Detection of Point Mutations Involving Tyrosine and Tryptophan. While the unfolded proteins show practically identical spectra in the amide I region, the infrared difference spectra reveal minor differences in the range 1300–1600 cm^{-1}. Such spectral differences were found between the spectra of the mutants Y45W and W59Y measured at 70 °C (see upper trace in Figure 7). The negative bands at 1516 and 1612 cm^{-1} can clearly be assigned to absorptions of tyrosine and therefore reflect the existence of two additional tyrosine residues in the latter mutant (i.e., 10 in W59Y versus 8 in Y45W). The sharp positive features in the difference spectrum at 1455 and 1334 cm^{-1} are assigned to infrared bands of tryptophan. There are two tryptophan residues in the mutant Y45W, but none in W59Y. To our knowledge, this is the first time that tryptophan side-chain modes in the range 1300–1500 cm^{-1} have been identified in the infrared spectrum of proteins. However, these tryptophan bands are much weaker than the tyrosine bands, and they also overlap strongly with other infrared bands, particularly with the strong band at 1455 cm^{-1}. It remains to be seen whether specific information on the microenvironment of tryptophan residues in proteins can be derived from an analysis of the corresponding infrared spectra in this spectral region.

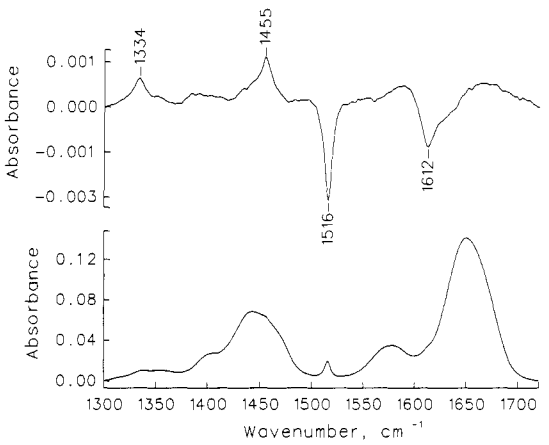

FIGURE 7: Upper trace: Infrared difference spectrum obtained by subtracting the absorbance spectrum of the mutant W59Y (0 Trp/10 Tyr) measured at 70 °C from that of the mutant Y45W (2 Trp/8 Tyr) measured at 70 °C. Lower trace: Absorbance spectrum of the mutant Y45W measured at 70 °C. Note that the *Y*-scale for the difference spectrum was expanded by a factor of 20 compared to the scale of the absorbance spectrum.

CONCLUDING REMARKS

The present data show that infrared spectroscopy permits a detailed analysis of the impact of point mutations on the structure and thermal stability of proteins. In the case of proteins whose thermal denaturation is reversible, the spectra of the thermally unfolded proteins provide an ideal internal intensity standard for the normalization of the spectra of the native proteins. In particular, while searching for structural differences among the folded states of the wild-type RNase T1 protein and its mutants, it was found that the major impact, as revealed by the corresponding infrared difference spectra, was the replacement of tryptophan in position 59 by tyrosine. This correlates very well with X-ray results and demonstrates the sensitivity of the infrared spectroscopic approach. In certain cases, infrared spectroscopy possibly even detects minor conformational differences that are not obvious from the X-ray analysis or could only be present in aqueous solution. The strategy discussed in this paper should find a wide range of applications in the comparative analysis of protein conformation.

REFERENCES

Arrondo, J. L. R., Young, N. M., & Mantsch, H. H. (1988) *Biochim. Biophys. Acta 952*, 261–268.

Braiman, M. S., & Rothschild, K. J. (1988) *Annu. Rev. Biophys. Biophys. Chem. 17*, 541–570.

Cameron, D. G., Kauppinen, J., Moffatt, D. J., & Mantsch, H. H. (1982) *Appl. Spectrosc. 36*, 245–250.

Chirgadze, Y. N., Fedorov, O. V., & Trushina, N. P. (1975) *Biopolymers 14*, 679–694.

Fabian, H., Schultz, C., Naumann, D., Landt, O., Hahn, U., & Saenger, W. (1993) *J. Mol. Biol. 232*, 967–981.

Grunert, H. P., Landt, O., Zirpel-Giesebrecht, M., Backmann, J., Heinemann, U., Saenger, W., & Hahn, U. (1993) *Protein Eng. 6*, 739–744.

Itoh, T., Tomita, K. I., Hakashima, T., Hiroaki, H., Uesugi, S. I., Nishikawa, S., Amisaki, T., Morioka, H., Ohtsuka, E., & Ikehara, M. (1991) *J. Biochem. (Tokyo) 110*, 677–680.

Koellner, G., Grunert, H. P., Landt, O., & Saenger, W. (1991) *Eur. J. Biochem. 201*, 199–202.

Kraulis, P. J. (1991) *J. Appl. Crystallogr. 28*, 946–950.

Landt, O., Grunert, H. P., & Hahn, U. (1990) *Gene 96*, 125–128.

Landt, O., Zirpel-Giesebrecht, M., Milde, A., & Hahn, U. (1992) *J. Biotechnol. 24*, 189–194.

Mantsch, H. H., Moffatt, D. J., & Casal, H. L. (1988) *J. Mol. Struct. 173*, 285–298.

Martinez-Oyanedel, J., Choe, H. W., Heinemann, U., & Saenger, W. (1991) *J. Mol. Biol. 222*, 335–352.

Miyazawa, T., & Blout, E. R. (1961) *J. Am. Chem. Soc. 83*, 712–719.

Muga, A., Mantsch, H. H., & Surewicz, W. K. (1991) *Biochemistry 30*, 7219–7224.

Pace, C. N., Heinemann, U., Hahn, U., & Saenger, W. (1991) *Angew. Chem., Int. Ed. Engl. 30*, 343–360.

Plaza del Pino, I. M., Pace, C. N, & Freire, E. (1992) *Biochemistry 31*, 11196–11202.

Schubert, W. D., Schluckebier, G., Backmann, J., Granzin, J., Kisker, C., Choe, H. W., Hahn, U., Pfeil, W., & Saenger, W. (1994) *Eur. J. Biochem. 220*, 527–534.

Surewicz, W. K., Mantsch, H. H., & Chapman, D. (1993) *Biochemistry 32*, 389–394.

Yamamoto, T., & Tasumi, M. (1991) *J. Mol. Struct. 242*, 235–244.

Yu, Y., Makhatadze, G. I., Pace, C. N., & Privalov, P. L. (1994) *Biochemistry 33*, 3312–3319.